

# Mixed QCD-EW corrections for Higgs leptonic decay via $HW^+W^-$ vertex

---

Chichuan Ma,<sup>a</sup> Yuxuan Wang,<sup>a</sup> Xiaofeng Xu,<sup>b</sup> Li Lin Yang,<sup>c</sup> Bin Zhou<sup>a</sup>

<sup>a</sup>*School of Physics and State Key Laboratory of Nuclear Physics and Technology,  
Peking University, Beijing 100871, China*

<sup>b</sup>*Institut für Theoretische Physik, Universität Bern, Sidlerstrasse 5, CH-3012 Bern, Switzerland*

<sup>c</sup>*Zhejiang Institute of Modern Physics, Department of Physics, Zhejiang University, Hangzhou 310027, China*

*E-mail:* [chichuanma@pku.edu.cn](mailto:chichuanma@pku.edu.cn), [wangyuxuan119@pku.edu.cn](mailto:wangyuxuan119@pku.edu.cn),  
[pkuxxf@gmail.com](mailto:pkuxxf@gmail.com), [yanglilin@zju.edu.cn](mailto:yanglilin@zju.edu.cn), [2028910235@pku.edu.cn](mailto:2028910235@pku.edu.cn)

**ABSTRACT:** We consider the two-loop corrections to the  $HW^+W^-$  vertex at order  $\alpha\alpha_s$ . We construct a canonical basis for the two-loop integrals using the Baikov representation and the intersection theory. By solving the  $\epsilon$ -form differential equations, we obtain fully analytic expressions for the master integrals in terms of multiple polylogarithms, which allow fast and accurate numeric evaluation for arbitrary configurations of external momenta. We apply our analytic results to the decay process  $H \rightarrow \nu_e e W$ , and study both the integrated and differential decay rates. Our results can also be applied to the Higgs production process via  $W$  boson fusion.

---

## Contents

<b>1</b>	<b>Introduction</b>	<b>2</b>
<b>2</b>	<b>Notations and lower-order results</b>	<b>3</b>
<b>3</b>	<b>The <math>HW^+W^-</math> vertex at two loops</b>	<b>4</b>
3.1	Canonical basis of the two-loop integrals	5
3.2	Solution to the canonical differential equations	7
<b>4</b>	<b>Application to the decay process</b>	<b>9</b>
4.1	Analytic results at NNLO	9
4.2	Numeric results	10
<b>5</b>	<b>Summary and Outlook</b>	<b>12</b>
<b>A</b>	<b>The canonical basis for the master integrals</b>	<b>13</b>

---

# 1 Introduction

After the discovery of the Higgs boson in 2012, one of the primary goals of current and future high energy collider experiments is the precision measurements of various Higgs properties. These include the Large Hadron Collider (LHC) and its future upgrade High-Luminosity LHC (HL-LHC) [1], as well as future electron-positron colliders such as the Circular Electron Position Collider (CEPC) [2], the Future Circular Collider (FCC-ee) [3] and the International Linear Collider (ILC) [4]. An important property of the Higgs boson is its coupling to weak gauge bosons, namely, the  $Z^0$  boson and the  $W^\pm$  boson. Their precision knowledge is crucial for verifying the spontaneous electroweak symmetry breaking mechanism and for exploring the nature of the Higgs sector. If the Higgs sector is more complicated than the simplest version assumed by the Standard Model (SM), e.g., if the Higgs boson is composite, these gauge couplings may differ from the SM value by a tiny amount. The precision measurement of these couplings will then help us to detect such small effects resulting from physics at higher scales.

With the current LHC data, the  $HZZ$  coupling and the  $HW^+W^-$  coupling have been measured with an uncertainty of 11% and 15%, respectively [5]. At HL-LHC, the precision is estimated to be about 1.5% and 1.7%, respectively [6]. At future electron-positron colliders, the precisions for these couplings can be greatly improved. For the  $HZZ$  coupling, the accuracy is estimated to be about 0.25% at the CEPC with a center-of-mass energy  $\sqrt{s} = 250$  GeV [2], and about 0.17% at the FCC-ee with  $\sqrt{s} = 365$  GeV [3]; while for the  $HW^+W^-$  coupling, the precision is estimated to be about 1.4% at the CEPC and about 0.43% at the FCC-ee. To get the most out of the future high precision data, it is necessary to provide accurate theoretical predictions for production and decay processes sensitive to these couplings. Those related to the  $HZZ$  vertex have been extensively studied in the literature [7–18]. In this paper, we concentrate on the  $HW^+W^-$  vertex, and study its higher order perturbative corrections within the SM.

To setup the context, we will consider the decay process  $H \rightarrow W^*W \rightarrow \nu_e e W$  in this paper, although our results can also be applied to the production process  $e^+e^- \rightarrow H\nu_e\bar{\nu}_e$ . The leading order (LO) results [19–21] and the next-to-leading order (NLO) electroweak (EW) corrections [7] for this decay process have been known many years ago. Beyond the NLO, contributions enhanced by the large top quark mass have been considered at two-loops [11, 13] and three-loops [12], albeit the assumption  $m_H > 2m_W$ . For a light Higgs boson, Ref. [14] reconsidered these calculations, and also gave predictions for the differential decay rates.

In this paper, we provide exact analytic results for the next-to-next-to-leading order (NNLO) mixed QCD-EW corrections to the  $HW^+W^-$  vertex at order  $\alpha\alpha_s$ . The analytic expressions are valid for arbitrary values of the external momenta. Hence it is applicable to cases where both  $W$  bosons are off-shell, and also to cases where

the large top mass approximation may not hold. We apply these analytic results to the Higgs decay process, and provide numeric predictions for both integrated and differential decay rates. These results will be useful for extracting the  $HW^+W^-$  coupling from future high precision experimental data.

This paper is organized as follows. In Section 2 we briefly introduce our notations and the LO and NLO results. In Section 3 we present the analytic calculation of the mixed QCD-EW corrections for the  $HW^+W^-$  vertex, with generic momenta configurations. In Section 4, we apply our analytic results to the  $H \rightarrow \nu_e e W$  decay process, and obtain numeric predictions. The summary and outlook come in Section 5, and we leave some lengthy expressions to the Appendix.

## 2 Notations and lower-order results

In this section we setup our notations and present the LO results as well as the NLO EW corrections for the partial decay width. In our calculation we will neglect masses of all light fermions except that of the top quark. At LO we assign the momenta as

$$H(P) \rightarrow W_\nu^{*\pm}(q) + W_\mu^\mp(p_3) \rightarrow \bar{\nu}_e^-(p_1) + e^\pm(p_2) + W_\mu^\mp(p_3). \quad (2.1)$$

The scalar products of the momenta lead to

$$\begin{aligned} P^2 &= m_H^2, & p_1^2 &= p_2^2 = 0, & p_3^2 &= m_W^2, \\ q^2 &= (p_1 + p_2)^2 = Q^2 = M_{e\nu}^2, & (p_2 + p_3)^2 &= M_{eW}^2. \end{aligned} \quad (2.2)$$

The LO partial decay width is then written as

$$\Gamma_{\text{LO}} = \sum_{\text{spin,color}} \int d\text{PS}_3 \frac{1}{2m_H} |M_{\text{LO}}|^2, \quad (2.3)$$

where the 3-body phase-space integration measure is given by

$$d\text{PS}_3 = \left( \prod_{i=1}^3 \frac{d^3 p_i}{(2\pi)^3} \frac{1}{2E_i} \right) (2\pi)^4 \delta^{(4)}(P - p_1 - p_2 - p_3). \quad (2.4)$$

In general the 3-body phase-space integral can be performed numerically with a Monte Carlo program, which will be useful when we compute differential decay widths. For the fully integrated decay width at LO, the phase space integral can be calculated analytically and we find

$$\begin{aligned} \Gamma_{\text{LO}} &= \frac{\alpha^2 m_H}{384\pi(2r)^4 s_W^4} \left[ (1 - 4r^2)(47 - 52r^2 + 32r^4) + 24(1 - 6r^2 + 4r^4) \log(2r) \right. \\ &\quad \left. + \frac{24r(5 - 8r^2 + 4r^4) \cos^{-1}(r(3 - 4r^2))}{\sqrt{1 - r^2}} \right], \end{aligned} \quad (2.5)$$

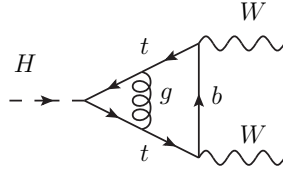


**Figure 1.** A typical Feynman diagram contributing to the mixed QCD-EW corrections for the  $HW^+W^-$  vertex.

where  $s_W = \sin\theta_W$  and  $r = m_H/(2m_W)$ . The NLO EW corrections to this decay process involve closed fermion loops, exchanges of electroweak gauge bosons and Higgs boson, as well as real photon emissions. For these corrections we invoke the program `MadGraph5_aMC@NLO` [22] which can automatically compute NLO QCD and EW corrections to standard model processes. In the rest of the paper, we present our calculation of the NNLO mixed QCD-EW corrections at order  $\alpha\alpha_s$ .

### 3 The $HW^+W^-$ vertex at two loops

In this section, we present the calculation of the two-loop form factors entering the mixed QCD-EW corrections for the  $HW^+W^-$  vertex. This serves as a main new result of this paper. A typical Feynman diagram is depicted in Fig. 1. The most generic Lorentz structure of the  $HW^+W^-$  vertex can be written as:

$$\mathcal{T}^{\mu\nu} = \frac{iem_W}{s_W} (g^{\mu\nu}T_1 + p_3^\mu p_3^\nu T_2 + p_3^\mu q^\nu T_3 + p_3^\nu q^\mu T_4 + q^\mu q^\nu T_5). \quad (3.1)$$

Among the scalar coefficient functions  $T_i$  in the above formula, only  $T_1$  and  $T_4$  contribute to the partial decay width. At NNLO, the coefficient functions can be written as linear combinations of scalar two-loop integrals of the form

$$F_{\{a_i\}} \equiv m_t^{4\epsilon} \int \frac{d^d k_1}{i\pi^{d/2}\Gamma(\epsilon)} \frac{d^d k_2}{i\pi^{d/2}\Gamma(\epsilon)} \prod_{i=1}^7 \frac{1}{D_i^{a_i}}, \quad (3.2)$$

where  $d = 4 - 2\epsilon$  in dimensional regularization,  $k_1$  and  $k_2$  are loop momenta, and  $\{a_i\} = \{a_1, a_2, a_3, a_4, a_5, a_6, a_7\}$  are the powers of propagator denominators  $D_i$  in the integrand. The propagator denominators are given by

$$\{k_1^2 - m_t^2, (k_1 - p_3 - q)^2 - m_t^2, k_2^2 - m_t^2, (k_2 - p_3 - q)^2 - m_t^2, (k_1 - q)^2, (k_2 - q)^2, (k_1 - k_2)^2\}.$$

The integrals can be reduced to a total of 38 master integrals via integration-by-parts (IBP) relations. For the reduction we utilize the program packages `FIRE` [23] and `LiteRed` [24].

To calculate the master integrals, we will employ the method of canonical differential equations [25–35]. For later convenience, we introduce the following dimensionless variables:

$$u = -\frac{m_H^2}{4m_t^2}, \quad v = -\frac{m_W^2}{4m_t^2}, \quad w = -\frac{Q^2}{4m_t^2}. \quad (3.3)$$

### 3.1 Canonical basis of the two-loop integrals

We would like to find linear combinations of integrals as in Eq. (3.2) which satisfy the canonical-form differential equations. Namely, the canonical basis  $\vec{f}(u, v, w; \epsilon)$  of the master integrals satisfy differential equations of the form

$$\begin{aligned} d\vec{f}(u, v, w; \epsilon) &= \epsilon dA(u, v, w) \vec{f}(u, v, w; \epsilon) \\ &= \epsilon \sum_i A_i d \log(\alpha_i) \vec{f}(u, v, w; \epsilon), \end{aligned} \quad (3.4)$$

where  $A_i$  are constant matrices independent of kinematic variables and the dimensional regulator. The “letters”  $\alpha_i \equiv \alpha_i(u, v, w)$  are algebraic functions of the kinematic variables  $u, v$  and  $w$ .

To find the canonical basis  $\vec{f}(u, v, w; \epsilon)$ , we use the method of [36] supplemented by suitable linear transformations to further simplify the differential equations. The method of [36] utilizes the Baikov representation [37] and look for  $d \log$ -form integrals which serve as candidates for the canonical basis. The Baikov representation for integrals of the form Eq. (3.2) can be written as

$$F_{\{a_i\}} = \mathcal{N}_\epsilon \int_{\mathcal{C}} u(\mathbf{z}) \frac{d^7 \mathbf{z}}{z_1^{a_1} z_2^{a_2} z_3^{a_3} z_4^{a_4} z_5^{a_5} z_6^{a_6} z_7^{a_7}}, \quad (3.5)$$

where  $z_i \equiv D_i$  are the propagator denominators which become integration variables in the Baikov representation, and the vector  $\mathbf{z}$  is the collection of  $z_i$ . The prefactor  $\mathcal{N}_\epsilon$  and the function  $u(\mathbf{z})$  are given by

$$\mathcal{N}_\epsilon = \frac{m_t^{4\epsilon} \lambda^{-1/2+\epsilon}}{4\pi^3 \Gamma(1-2\epsilon) \Gamma^2(\epsilon)}, \quad u(\mathbf{z}) = [P_0(\mathbf{z})]^{-1/2-\epsilon}, \quad P_0(\mathbf{z}) = G(k_1, k_2, p_3, q), \quad (3.6)$$

where  $\lambda \equiv \lambda(m_H^2, m_W^2, Q^2)$ , with  $\lambda(x, y, z) \equiv x^2 + y^2 + z^2 - 2xy - 2yz - 2zx$  being the Källén function. The Gram determinant is defined by

$$G(q_1, \dots, q_n) \equiv \det(-q_i \cdot q_j) \equiv \det \begin{pmatrix} -q_1 \cdot q_1 & -q_1 \cdot q_2 & \cdots & -q_1 \cdot q_n \\ -q_2 \cdot q_1 & -q_2 \cdot q_2 & & \vdots \\ \vdots & & \ddots & \vdots \\ -q_n \cdot q_1 & \cdots & \cdots & -q_n \cdot q_n \end{pmatrix}. \quad (3.7)$$

The integration domain  $\mathcal{C}$  in Eq. (3.5) has the property that  $u(\mathbf{z})$  vanishes on its boundary  $\partial\mathcal{C}$ .

For illustration purposes, we consider the  $\{1, 0, 1, 1, 1, 0, 1\}$  sub-topology, which turns out to be the most complicated one. This includes all integrals of the form Eq. (3.5) with the powers  $a_1, a_3, a_4, a_5$  and  $a_7$  being positive, and the powers  $a_2$  and  $a_6$  being non-positive. For the construction of  $d\log$ -form integrals, it is reasonable to first consider the cases where either  $a_2$  or  $a_6$  is fixed to zero. As an example, we will fix  $a_2 = 0$ . It is then possible to perform the integration over  $z_2$  in Eq. (3.5), resulting in

$$\mathcal{N}_\epsilon \int_{\mathcal{C}} u(\mathbf{z}) dz_2 \equiv \mathcal{N}'_\epsilon u_2(\mathbf{z}') = \mathcal{N}'_\epsilon P_1^{-1/2+\epsilon} P_2^{-\epsilon} P_3^{-\epsilon}, \quad (3.8)$$

where  $\mathbf{z}'$  is given by  $\mathbf{z}$  with  $z_2$  removed. The new prefactor and the polynomials are given by

$$\begin{aligned} \mathcal{N}'_\epsilon &= \frac{m_t^{4\epsilon} \lambda^{-1/2+\epsilon}}{4\pi^2 \Gamma^2(1-\epsilon) \Gamma^2(\epsilon)}, \\ P_1 &= P_1(z_3, z_6) = -4G(k_2, q), \\ P_2 &= P_2(z_1, z_3, z_5, z_7, z_6) = 4G(k_1, k_2, q), \\ P_3 &= P_3(z_3, z_4, z_6) = 4G(k_2, p_3, q). \end{aligned} \quad (3.9)$$

The integrals in this sub-topology with  $a_2 = 0$  can then be expressed as

$$F_{\{a_i\}} = \mathcal{N}'_\epsilon \int_{\mathcal{C}} u_2(\mathbf{z}') \frac{d^6 \mathbf{z}'}{z_1^{a_1} z_3^{a_3} z_4^{a_4} z_5^{a_5} z_6^{a_6} z_7^{a_7}}, \quad (3.10)$$

which is equivalent to a loop-by-loop Baikov representation.

We now want to search for rational functions  $\hat{\varphi}(\mathbf{z}')$  such that the integrand  $u_2(\mathbf{z}')\hat{\varphi}(\mathbf{z}')$  takes the  $d$ -dimensional generalized  $d\log$ -form [36]. We perform the construction in the variable-by-variable approach in the order  $z_6, z_1, z_5, z_3, z_4, z_7$ , and find 4 candidates for the canonical Feynman integrals in this sub-topology:

$$\begin{aligned} \hat{\varphi}_1 &= \frac{\sqrt{\lambda}}{z_1 z_3 z_4 z_5 z_7}, \\ \hat{\varphi}_2 &= \frac{\sqrt{\lambda} \sqrt{m_H^2 (m_H^2 - 4m_t^2)}}{z_1 z_3 z_4 z_5 z_7} \frac{1}{P_3} \frac{\partial P_3}{\partial z_4}, \\ \hat{\varphi}_3 &= \frac{1}{z_1 z_3 z_4 z_5 z_7} \left[ \frac{1}{P_3} \frac{\partial P_3}{\partial z_4} \frac{\partial P_3}{\partial z_6} - 2 \frac{\partial^2 P_3}{\partial z_4 \partial z_6} \right], \\ \hat{\varphi}_4 &= \frac{\sqrt{\lambda} (Q^2 - m_t^2)}{z_1 z_3 z_4 z_5 z_7} \frac{1}{P_2} \frac{\partial P_2}{\partial z_5}. \end{aligned} \quad (3.11)$$

These candidates can be converted to Feynman integrals of the form (3.5) using intersection theory [38–44] or via IBP relations. The results are given by

$$\begin{aligned}
\varphi_1 &= -\frac{16m_t^4 R_1 R_2}{\epsilon} F_{1,0,1,2,1,0,1}, \\
\varphi_2 &= -\frac{4m_t^2(u+v-w)}{\epsilon} F_{0,2,1,0,0,1,1} - 8m_t^2(u-v+w) F_{1,0,1,1,1,0,1} \\
&\quad - \frac{8m_t^4 u(2u-2v-2w+1)}{\epsilon} F_{1,0,1,2,1,0,1} + \frac{8m_t^2 u}{\epsilon} F_{1,0,1,2,1,-1,1}, \\
\varphi_3 &= \frac{4m_t^4(4w+1)R_2}{\epsilon} F_{1,0,1,1,2,0,1}, \\
\varphi_4 &= -\frac{16m_t^4 w R_2}{\epsilon} F_{2,0,1,1,1,1,0} - \frac{2m_t^2 R_2}{\epsilon} F_{0,2,1,1,0,1,0}.
\end{aligned} \tag{3.12}$$

Where we have introduced the following two square roots:

$$R_1 \equiv R_1(u) = \sqrt{u(u+1)}, \quad R_2 \equiv R_2(u, v, w) = \sqrt{\lambda(u, v, w)}. \tag{3.13}$$

Applying the same procedure to other (sub)-topologies, we are able to construct 38  $d \log$ -form integrals in the Baikov representation, and convert them to Feynman integrals using either traditional IBP method or the intersection theory. We have checked that they indeed satisfy the canonical-form differential equations (3.4). Further (simple) linear transforms can be applied to simplify the matrices  $A_i$ . The final form of the canonical basis  $\vec{f}(u, v, w; \epsilon)$  in terms of linear combinations of Feynman integrals is given in Appendix A.

### 3.2 Solution to the canonical differential equations

The differential equations (3.4) involve 18 independent letters as following:

$$\left\{ u, \frac{R_1 - u}{R_1 + u}, u + 1, v, 4v + 1, w, 4w + 1, \lambda(u, v, w), \right. \\
\frac{v - w - R_1 - R_2}{v - w + R_1 - R_2}, \frac{v - w + R_1 - R_2}{v - w - R_1 + R_2}, \frac{v - w - R_1 - R_2}{v - w + R_1 + R_2}, \\
\frac{u + v - w - R_2}{u + v - w + R_2}, \frac{u - v + w - R_2}{u - v + w + R_2}, \frac{2R_2 + g(u, v, w)}{2R_2 - g(u, v, w)}, \frac{2R_2 + g(u, w, v)}{2R_2 - g(u, w, v)}, \\
\left. h(u, v, w), h(u, w, v), 4(v - w)^2 - u(4v + 1)(4w + 1) \right\}, \tag{3.14}$$

where we have introduced the following polynomials:

$$g(u, v, w) = 1 + 2u + 2v - 2w,$$

$$h(u, v, w) = 1 + 4u + 4v + 16uv - 4w, \quad (3.15)$$

The solution to the canonical form differential equations (3.4) can be formally written as a path-ordered exponential integrated from the boundary point  $\vec{x}_0 = (u_0, v_0, w_0)$  to the point  $\vec{x} = (u, v, w)$

$$\vec{f}(u, v, w; \epsilon) = \mathcal{P} \exp \left( \epsilon \int_{\vec{x}_0}^{\vec{x}} dA \right) \vec{f}(u_0, v_0, w_0; \epsilon). \quad (3.16)$$

We choose the boundary point to be  $\vec{x}_0 = (0, 0, 0)$ , which corresponds to zero external momenta. The values of the mater integrals at the boundary can be easily obtained and are given by

$$\begin{aligned} f_1(0, 0, 0; \epsilon) &= 1, \\ f_5(0, 0, 0; \epsilon) &= f_7(0, 0, 0; \epsilon) = -\frac{\Gamma(1-\epsilon)\Gamma(1+2\epsilon)}{\Gamma(1+\epsilon)}, \\ f_{22}(0, 0, 0; \epsilon) &= f_{25}(0, 0, 0; \epsilon) = \frac{1}{8} - \frac{\Gamma(1-\epsilon)\Gamma(2\epsilon)}{4\Gamma(\epsilon)}, \end{aligned} \quad (3.17)$$

with  $f_i(0, 0, 0; \epsilon) = 0$  for all other  $i$ 's.

The path-ordered exponential (3.16) can be expanded as power series in  $\epsilon$ . At each order in  $\epsilon$  we need to evaluate iterated integrals in terms of generalized polylogarithms (GPLs) [45]. For that it is convenient to perform a change of variables such that the integration kernels are rational functions without square roots. There are two ways to achieve that, which lead to the same final results. The first is to perform variable changes on  $u$ ,  $v$  and  $w$ , such that both  $R_1$  and  $R_2$  become rational functions of the new variables. This can be done using the method of [46, 47]. The second way, which we'll describe in more details, amounts to choosing a specific integration path in the  $(u, v, w)$  space, such that the integration reduces to a single-variable problem. Observing that  $R_2$  is homogeneous in  $u$ ,  $v$  and  $w$ , it is reasonable to pick a straight path from  $(0, 0, 0)$  to  $(u, v, w)$  parameterized by a variable  $t$  as  $(tu, tv, tw)$ . During the integration over  $t$ ,  $R_2$  simply becomes  $t$  multiplied by a constant factor:

$$R_2(tu, tv, tw) = tR_2(u, v, w). \quad (3.18)$$

On the other hand, we now need to perform a variable change on  $t$  such that  $R_1(tu)$  becomes a rational function. This can be simply done with

$$t = \frac{x^2}{4u(1-x)}, \quad R_1(tu) = \frac{x(x-2)}{4(x-1)}. \quad (3.19)$$

When  $t$  goes from 0 to 1,  $x$  goes from 0 to  $2(R_1(u) - u)$ . This determines the integration domain over  $x$ .

After the variable change, the iterated integrals at order  $\epsilon^n$  have the generic structure

$$\int dx \frac{1}{x - x_i} G^{(n-1)}(x), \quad (3.20)$$

with  $G^{(n-1)}(x)$  being functions at order  $\epsilon^{n-1}$ . These integrals can be naturally evaluated in terms of GPLs, with the branch points  $x_i$  given by

$$\begin{aligned} x_1 &= 1, & x_2 &= 2, & x_3 &= 0, & x_4 &= \frac{u + v - w + R_2}{2v}, & x_5 &= \frac{u + v - w - R_2}{2v}, \\ x_6 &= \frac{u - v + w + R_2}{2w}, & x_7 &= \frac{u - v + w - R_2}{2w}, & x_8 &= \frac{u - \sqrt{u(u - 4v)}}{2v}, \\ x_9 &= \frac{u + \sqrt{u(u - 4v)}}{2v}, & x_{10} &= \frac{u - \sqrt{u(u - 4v)}}{2w}, & x_{11} &= \frac{u + \sqrt{u(u - 4w)}}{2w}, \\ x_{12} &= \frac{u + \sqrt{u(2v - 2w - u + 2R_2)}}{u - v + w - R_2}, & x_{13} &= \frac{u - \sqrt{u(2v - 2w - u + 2R_2)}}{u - v + w - R_2}, \\ x_{14} &= \frac{u + \sqrt{u(2w - 2v - u + 2R_2)}}{u + v - w - R_2}, & x_{15} &= \frac{u - \sqrt{u(2w - 2v - u + 2R_2)}}{u + v - w - R_2}, \\ x_{16} &= \frac{u - \sqrt{u(2w - 2v - u - 2R_2)}}{u + v - w + R_2}, & x_{17} &= \frac{u + \sqrt{u(2w - 2v - u - 2R_2)}}{u + v - w + R_2}, \\ x_{18} &= \frac{u - \sqrt{u(2v - 2w - u - 2R_2)}}{u - v + w + R_2}, & x_{19} &= \frac{u + \sqrt{u(2v - 2w - u - 2R_2)}}{u - v + w + R_2}. \end{aligned} \quad (3.21)$$

The resulting GPLs can be evaluated numerically using program libraries `GiNaC` [48–50] and `handyG` [51]. We have checked that our results for the master integrals are in good agreement with the numeric results of `pySecDec` [52].

## 4 Application to the decay process

### 4.1 Analytic results at NNLO

In this section, we apply the two-loop integrals calculated in the previous section to the decay process  $H \rightarrow e\nu_e W$  at order  $\alpha\alpha_s$ . The decay process receives three kinds of contributions at this order: the corrections to the  $HW^+W^-$  vertex, the corrections to the propagator of the off-shell  $W^\pm$  field, and the corrections to the  $e\nu_e W$  vertex (arising from counter-terms). In practice these can all be described by their contributions to the coefficient functions in Eq. (3.1) (with the third kind of contributions only affecting  $T_1$ ). The squared amplitude at this order can then be written as

$$2\Re(M_{\text{LO}}^* M_{\alpha\alpha_s}) = \frac{8\pi^2\alpha^2}{s_W^4 (M_{e\nu}^2 - m_W^2)^2} \left[ \Re(T_4) (M_{e\nu}^2 - m_H^2 + m_W^2) \right]$$

$$\begin{aligned}
& \times (M_{e\nu}^2 M_{eW}^2 + (M_{eW}^2 - m_H^2)(M_{eW}^2 - m_W^2)) \\
& - 2\Re(T_1) (M_{e\nu}^2(M_{eW}^2 - 2m_W^2) + (M_{eW}^2 - m_H^2)(M_{eW}^2 - m_W^2)) \Big].
\end{aligned} \tag{4.1}$$

To calculate the coefficient functions, we generate the relevant Feynman diagrams using `FeynArts` [53]. The resulting amplitudes are further manipulated with `Mathematica`. In addition to the Feynman integrals calculated in the previous section, we also need to calculate a couple of extra integrals arising in the  $W^\pm$  propagator and in the counter-terms. We have checked these results against those in the literature [54, 55].

We renormalize the fields and the masses in the on-shell scheme, with pole masses  $m_W$ ,  $m_Z$ ,  $m_H$  and  $m_t$  as input parameters. The weak mixing angle is defined by the on-shell relation  $c_W \equiv \cos(\theta_W) = m_W/m_Z$ , whose renormalization is given by  $\delta c_W^2/c_W^2 = \delta m_W^2/m_W^2 - \delta m_Z^2/m_Z^2$ . For the renormalization of the fine structure constant  $\alpha$ , we choose two different schemes: the  $\alpha(m_Z)$ -scheme with  $\alpha(m_Z) = \alpha(0)/(1 - \Delta\alpha(m_Z))$  as the input parameter, where  $\Delta\alpha(m_Z)$  encodes the contributions to the renormalization of  $\alpha$  from light fermion loops (including leptons and 5 flavors of light quarks); and the  $G_\mu$ -scheme with the Fermi-constant  $G_\mu$  determined from the muon decay data as the input parameter. In the  $G_\mu$ -scheme, the coupling is given by

$$\alpha_{G_\mu} = \frac{\sqrt{2}}{\pi} G_\mu m_W^2 \left( 1 - \frac{m_W^2}{m_Z^2} \right). \tag{4.2}$$

## 4.2 Numeric results

We now present the numeric predictions from our calculations. We choose the input parameters as  $m_t = 172.76$  GeV,  $m_H = 125.1$  GeV,  $m_Z = 91.1876$  GeV,  $m_W = 80.379$  GeV,  $G_\mu = 1.1663787 \times 10^{-5}$  GeV<sup>-2</sup>,  $\alpha(m_Z) = 1/128.929$  and  $\alpha_s(m_Z) = 0.1179$  [56]. The default renormalization scale for  $\alpha_s$  is chosen as  $\mu = m_H$ .

In Table 1 and Table 2, we show the LO, NLO EW, and NNLO QCD-EW predictions to the partial decay widths in the  $\alpha(m_Z)$ -scheme and  $G_\mu$ -scheme, respectively. We find that the mixed QCD-EW corrections amount to about 1% of the LO prediction in the  $\alpha(m_Z)$ -scheme, and about 0.2% of the LO prediction in the  $G_\mu$ -scheme. The smallness of the contributions in the  $G_\mu$ -scheme can be partly attributed to the fact that corrections to the  $W$  propagator and to the  $e\nu_e W$  vertex are absorbed into the coupling constant. Nevertheless, we find that the NNLO results in the two schemes are rather close to each other, showing the stability of our prediction against scheme changes.

We now proceed to study the differential decay rates. In Fig. 2 we depict the  $M_{e\nu}$  distribution at various orders in perturbation theory, in the two renormalization schemes mentioned above. This distribution gives us information about the virtuality

	LO	NLO EW	NNLO QCD-EW
$\Gamma$ ( $10^{-5}$ GeV)	4.597	4.474	4.518
$\delta\Gamma$ ( $10^{-5}$ GeV)		-0.123	+0.044
$\delta\Gamma/\Gamma_{\text{LO}}$		-2.7%	+1.0%

**Table 1.** The partial decay widths at various orders in the  $\alpha(m_Z)$  scheme.

	LO	NLO EW	NNLO QCD-EW
$\Gamma$ ( $10^{-5}$ GeV)	4.374	4.524	4.531
$\delta\Gamma$ ( $10^{-5}$ GeV)		+0.150	+0.007
$\delta\Gamma/\Gamma_{\text{LO}}$		+3.4%	+0.2%

**Table 2.** The partial decay widths at various orders in the  $G_\mu$  scheme.

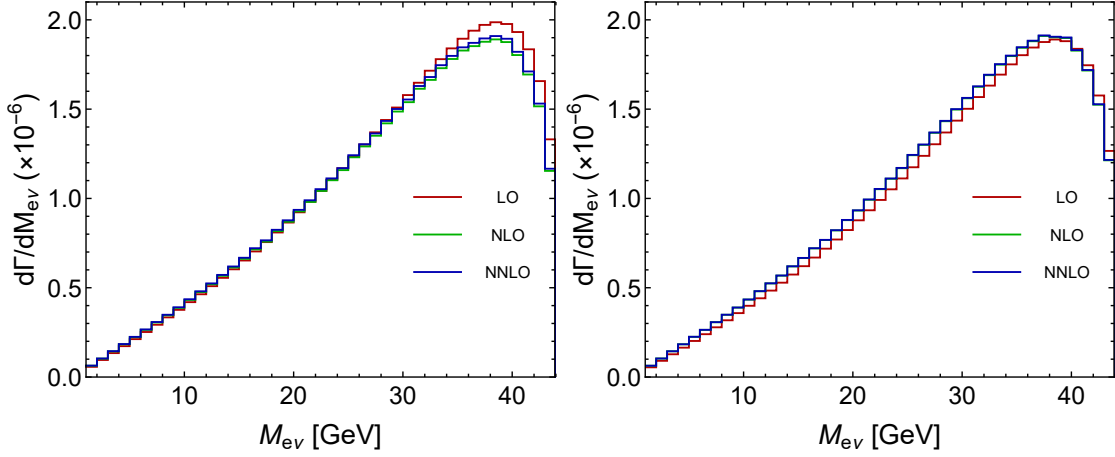


**Figure 2.** The  $M_{e\nu}$  distribution in the  $\alpha(m_Z)$  scheme (left) and in the  $G_\mu$  scheme (right).

of the off-shell  $W$  boson. Here we observe similar behaviors as for the integrated decay rate. The NNLO corrections are much smaller in the  $G_\mu$  scheme, as shown in the right plot in Fig. 2, where the green and blue curves almost completely overlap with each other. Since the neutrino is not observable (although could be reconstructed), it is also interesting to study the invariant mass of the visible part of the decay products. In Fig. 3 we show the  $M_{eW}$  distribution, again in the two schemes at different orders. This distribution can be measured at the LHC and the future Higgs factories, with the  $W$  boson decaying hadronically. Our results then provide the high precision theoretical predictions to be compared with the experimental data.

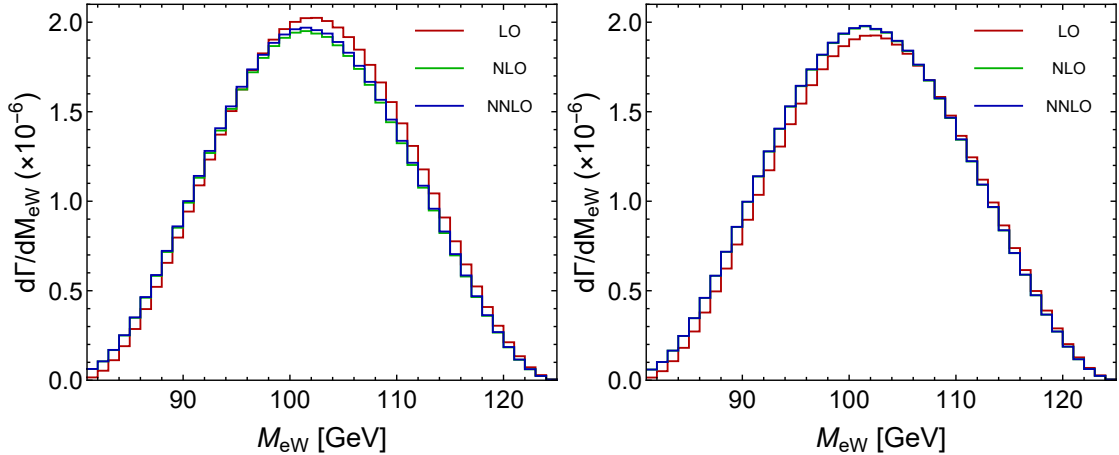


**Figure 3.** The  $M_{eW}$  distribution in the  $\alpha(m_Z)$  scheme (left) and in the  $G_\mu$  scheme (right).

## 5 Summary and Outlook

In this paper, we have studied a class of two-loop triangle integrals entering the  $\mathcal{O}(\alpha\alpha_s)$  corrections to the  $HW^+W^-$  vertex. We have constructed a canonical basis consisting of 38 master integrals using the Baikov representation and intersection theory. We have derived the  $\epsilon$ -form differential equations for the master integrals, and are able to find fully analytic solutions in terms of GPLs. The fully analytic form allows fast and accurate numeric evaluation for any combination of external momenta and internal masses, which is important for phenomenological studies.

We apply our results to the  $H \rightarrow \nu_e e W$  decay process. For the integrated decay width, we find that the NNLO mixed QCD-EW corrections can reach 1% of the LO result in the  $\alpha(m_Z)$  scheme. The size of the corrections are reduced to about 0.2% in the  $G_\mu$  scheme. This seems to indicate that the perturbative convergence in the  $G_\mu$  scheme is better. However, this needs to be confirmed by the behavior of the purely electroweak two-loop corrections of order  $\alpha^2$ . We have also studied the differential decay rates and drawn similar conclusions.

For the decay process, the complete  $\mathcal{O}(\alpha\alpha_s)$  corrections are not expected to be quite different in size compared to those calculated in the heavy top limit [11–14]. However, the fully analytic form of our results enable us to study cases where the virtuality of  $W^\pm$  bosons exceeds the top quark mass, where the heavy top approximation is no longer valid. This is the case for, e.g., the  $W$  boson fusion process  $W^{+*}W^{-*} \rightarrow H$ . The  $\mathcal{O}(\alpha\alpha_s)$  corrections for this production process will be presented in a forthcoming article.

## A The canonical basis for the master integrals

In this appendix, we provide the canonical basis for the master integrals appearing in the  $\mathcal{O}(\alpha_s)$  corrections to the  $HW^+W^-$  vertex. The 38 integrals are given by

$$f_1 = F_{0,2,0,2,0,0,0},$$

$$f_2 = um_t^2 F_{0,2,2,0,0,0,1},$$

$$f_3 = 2m_t^2 R_1 F_{0,2,1,0,0,0,2} + m_t^2 R_1 F_{0,2,2,0,0,0,1},$$

$$f_4 = vm_t^2 F_{0,0,0,2,2,0,1},$$

$$f_5 = (4v + 1)m_t^2 F_{0,0,0,1,2,0,2} + 2m_t^2 F_{0,0,0,2,2,0,1},$$

$$f_6 = wm_t^2 F_{0,0,2,0,2,0,1},$$

$$f_7 = (4w + 1)m_t^2 F_{0,0,1,0,2,0,2} + 2m_t^2 F_{0,0,2,0,2,0,1},$$

$$f_8 = m_t^2 R_1 F_{0,2,1,2,0,0,0},$$

$$f_9 = vm_t^2 F_{0,2,0,2,0,1,0},$$

$$f_{10} = wm_t^2 F_{0,2,2,0,0,1,0},$$

$$f_{11} = m_t^4 R_1^2 F_{2,1,2,1,0,0,0},$$

$$f_{12} = v^2 m_t^4 F_{0,2,0,2,1,1,0},$$

$$f_{13} = w^2 m_t^4 F_{2,0,2,0,1,1,0},$$

$$f_{14} = vwm_t^4 F_{0,2,2,0,1,1,0},$$

$$f_{15} = wm_t^4 R_1 F_{2,0,2,1,1,0,0},$$

$$f_{16} = vm_t^4 R_1 F_{0,2,2,1,1,0,0},$$

$$f_{17} = \epsilon m_t^2 R_2 F_{0,2,1,1,0,1,0},$$

$$f_{18} = \epsilon m_t^2 R_2 F_{0,0,1,1,2,0,1},$$

$$f_{19} = m_t^2 R_1 (\epsilon F_{0,0,1,1,2,0,1} + (2\epsilon - 1)(F_{0,0,1,2,1,0,1} + F_{0,0,2,1,1,0,1})),$$

$$f_{20} = \epsilon m_t^2 R_2 F_{0,1,1,0,1,0,2},$$

$$f_{21} = \epsilon m_t^2 R_2 F_{0,1,2,0,1,0,1},$$

$$f_{22} = -\frac{1}{4}m_t^2 (\epsilon(F_{0,1,1,0,1,0,2} + 2F_{0,1,2,0,1,0,1})g(u, v, w) + F_{0,2,2,0,1,0,1}m_t^2 h(u, v, w)),$$

$$\begin{aligned}
f_{23} &= \epsilon m_t^2 R_2 F_{0,1,1,0,0,1,2}, \\
f_{24} &= \epsilon m_t^2 R_2 F_{0,2,1,0,0,1,1}, \\
f_{25} &= -\frac{1}{4} m_t^2 (\epsilon (F_{0,1,1,0,0,1,2} + 2F_{0,2,1,0,0,1,1}) g(u, w, v) + F_{0,2,2,0,0,1,1} m_t^2 h(u, w, v)), \\
f_{26} &= \epsilon m_t^4 R_1 R_2 F_{2,1,1,1,0,1,0}, \\
f_{27} &= v \epsilon m_t^4 R_2 F_{0,2,1,1,1,1,0}, \\
f_{28} &= w \epsilon m_t^4 R_2 F_{2,0,1,1,1,1,0}, \\
f_{29} &= \epsilon^2 m_t^2 R_2 F_{0,1,1,0,1,1,1}, \\
f_{30} &= \epsilon^2 m_t^2 R_2 F_{1,0,1,1,1,0,1}, \\
f_{31} &= \epsilon m_t^4 R_1 R_2 F_{1,0,1,2,1,0,1}, \\
f_{32} &= -\epsilon^2 m_t^2 (u - v + w) F_{1,0,1,1,1,0,1} - \epsilon m_t^4 u (2u - 2v - 2w + 1) F_{1,0,1,2,1,0,1} \\
&\quad - \frac{1}{2} \epsilon m_t^2 (u + v - w) F_{0,2,1,0,0,1,1} + \epsilon m_t^2 u F_{1,0,1,2,1,-1,1}, \\
f_{33} &= (4w + 1) \epsilon m_t^4 R_2 F_{1,0,1,1,2,0,1}, \\
f_{34} &= \epsilon^2 m_t^2 R_2 F_{0,1,1,1,1,0,1}, \\
f_{35} &= \epsilon m_t^4 R_1 R_2 F_{0,1,2,1,1,0,1}, \\
f_{36} &= -\epsilon^2 m_t^2 (u + v - w) F_{0,1,1,1,1,0,1} - \epsilon m_t^4 u (2u - 2v - 2w + 1) F_{0,1,2,1,1,0,1} \\
&\quad - \frac{1}{2} \epsilon m_t^2 (u - v + w) F_{0,1,2,0,1,0,1} + \epsilon m_t^2 u F_{0,1,2,1,1,-1,1}, \\
f_{37} &= (4v + 1) \epsilon m_t^4 R_2 F_{0,1,1,1,2,0,1}, \\
f_{38} &= \epsilon^2 m_t^4 R_2^2 F_{1,1,1,1,1,1,0}.
\end{aligned}$$

where  $u, v, w, R_1$  and  $R_2$  are defined by Eq. (3.3) and Eq. (3.13), respectively, and the functions  $g(u, v, w)$  and  $h(u, v, w)$  are given in Eq. (3.15).

## References

- [1] G. Apollinari, O. Brüning, T. Nakamoto and L. Rossi, *High Luminosity Large Hadron Collider HL-LHC*, [1705.08830](#).
- [2] CEPC STUDY GROUP collaboration, *CEPC Conceptual Design Report: Volume 2 - Physics & Detector*, [1811.10545](#).

- [3] FCC collaboration, *FCC Physics Opportunities: Future Circular Collider Conceptual Design Report Volume 1*, *Eur. Phys. J. C* **79** (2019) 474.
- [4] P. Bambade et al., *The International Linear Collider: A Global Project*, [1903.01629](#).
- [5] CMS collaboration, *Combined measurements of Higgs boson couplings in proton–proton collisions at  $\sqrt{s} = 13$  TeV*, *Eur. Phys. J. C* **79** (2019) 421 [[1809.10733](#)].
- [6] M. Cepeda et al., *Report from Working Group 2: Higgs Physics at the HL-LHC and HE-LHC*, *CERN Yellow Rep. Monogr.* **7** (2019) 221 [[1902.00134](#)].
- [7] J. Fleischer and F. Jegerlehner, *Radiative Corrections to Higgs Decays in the Extended Weinberg-Salam Model*, *Phys. Rev. D* **23** (1981) 2001.
- [8] J. Fleischer and F. Jegerlehner, *Radiative Corrections to Higgs Production by  $e^+e^- \rightarrow ZH$  in the Weinberg-Salam Model*, *Nucl. Phys. B* **216** (1983) 469.
- [9] B.A. Kniehl, *Radiative corrections for associated  $ZH$  production at future  $e^+e^-$  colliders*, *Z. Phys. C* **55** (1992) 605.
- [10] A. Denner, J. Kublbeck, R. Mertig and M. Bohm, *Electroweak radiative corrections to  $e^+e^- \rightarrow HZ$* , *Z. Phys. C* **56** (1992) 261.
- [11] B.A. Kniehl, *Two loop  $O(\alpha_s G(F) M(Q)^2)$  heavy quark corrections to the interactions between Higgs and intermediate bosons*, *Phys. Rev. D* **53** (1996) 6477 [[hep-ph/9602304](#)].
- [12] A. Frink, B.A. Kniehl, D. Kreimer and K. Riesselmann, *Heavy Higgs lifetime at two loops*, *Phys. Rev. D* **54** (1996) 4548 [[hep-ph/9606310](#)].
- [13] A. Djouadi, P. Gambino and B.A. Kniehl, *Two loop electroweak heavy fermion corrections to Higgs boson production and decay*, *Nucl. Phys. B* **523** (1998) 17 [[hep-ph/9712330](#)].
- [14] B.A. Kniehl and O.L. Veretin, *Low-mass Higgs decays to four leptons at one loop and beyond*, *Phys. Rev. D* **86** (2012) 053007 [[1206.7110](#)].
- [15] Y. Gong, Z. Li, X. Xu, L.L. Yang and X. Zhao, *Mixed QCD-EW corrections for Higgs boson production at  $e^+e^-$  colliders*, *Phys. Rev. D* **95** (2017) 093003 [[1609.03955](#)].
- [16] Q.-F. Sun, F. Feng, Y. Jia and W.-L. Sang, *Mixed electroweak-QCD corrections to  $e^+e^- \rightarrow HZ$  at Higgs factories*, *Phys. Rev. D* **96** (2017) 051301 [[1609.03995](#)].
- [17] W. Chen, F. Feng, Y. Jia and W.-L. Sang, *Mixed electroweak-QCD corrections to  $e^+e^- \rightarrow \mu^+\mu^-H$  at CEPC with finite-width effect*, *Chin. Phys. C* **43** (2019) 013108 [[1811.05453](#)].
- [18] Y. Wang, X. Xu and L.L. Yang, *Two-loop triangle integrals with 4 scales for the  $HZV$  vertex*, *Phys. Rev. D* **100** (2019) 071502 [[1905.11463](#)].
- [19] T.G. Rizzo, *Decays of Heavy Higgs Bosons*, *Phys. Rev. D* **22** (1980) 722.

- [20] G. Pocsik and T. Torma, *On the Decays of Heavy Higgs Bosons*, *Z. Phys. C* **6** (1980) 1.
- [21] W.-Y. Keung and W.J. Marciano, *HIGGS SCALAR DECAYS:  $H \rightarrow W^+ X$* , *Phys. Rev. D* **30** (1984) 248.
- [22] R. Frederix, S. Frixione, V. Hirschi, D. Pagani, H.S. Shao and M. Zaro, *The automation of next-to-leading order electroweak calculations*, *JHEP* **07** (2018) 185 [[1804.10017](#)].
- [23] A.V. Smirnov and F.S. Chuharev, *FIRE6: Feynman Integral REduction with Modular Arithmetic*, *Comput. Phys. Commun.* **247** (2020) 106877 [[1901.07808](#)].
- [24] R.N. Lee, *LiteRed 1.4: a powerful tool for reduction of multiloop integrals*, *J. Phys. Conf. Ser.* **523** (2014) 012059 [[1310.1145](#)].
- [25] A.V. Kotikov, *Differential equations method: New technique for massive Feynman diagrams calculation*, *Phys. Lett. B* **254** (1991) 158.
- [26] A.V. Kotikov, *Differential equation method: The Calculation of  $N$  point Feynman diagrams*, *Phys. Lett. B* **267** (1991) 123.
- [27] E. Remiddi, *Differential equations for Feynman graph amplitudes*, *Nuovo Cim. A* **110** (1997) 1435 [[hep-th/9711188](#)].
- [28] T. Gehrmann and E. Remiddi, *Differential equations for two loop four point functions*, *Nucl. Phys. B* **580** (2000) 485 [[hep-ph/9912329](#)].
- [29] M. Argeri and P. Mastrolia, *Feynman Diagrams and Differential Equations*, *Int. J. Mod. Phys. A* **22** (2007) 4375 [[0707.4037](#)].
- [30] S. Müller-Stach, S. Weinzierl and R. Zayadeh, *Picard-Fuchs equations for Feynman integrals*, *Commun. Math. Phys.* **326** (2014) 237 [[1212.4389](#)].
- [31] J.M. Henn, *Multiloop integrals in dimensional regularization made simple*, *Phys. Rev. Lett.* **110** (2013) 251601 [[1304.1806](#)].
- [32] J.M. Henn, *Lectures on differential equations for Feynman integrals*, *J. Phys. A* **48** (2015) 153001 [[1412.2296](#)].
- [33] J. Ablinger, A. Behring, J. Blümlein, A. De Freitas, A. von Manteuffel and C. Schneider, *Calculating Three Loop Ladder and V-Topologies for Massive Operator Matrix Elements by Computer Algebra*, *Comput. Phys. Commun.* **202** (2016) 33 [[1509.08324](#)].
- [34] L. Adams, E. Chaubey and S. Weinzierl, *Simplifying Differential Equations for Multiscale Feynman Integrals beyond Multiple Polylogarithms*, *Phys. Rev. Lett.* **118** (2017) 141602 [[1702.04279](#)].
- [35] J. Bosma, K.J. Larsen and Y. Zhang, *Differential equations for loop integrals in Baikov representation*, *Phys. Rev. D* **97** (2018) 105014 [[1712.03760](#)].
- [36] J. Chen, X. Jiang, X. Xu and L.L. Yang, *Constructing canonical Feynman integrals with intersection theory*, *Phys. Lett. B* **814** (2021) 136085 [[2008.03045](#)].

- [37] P.A. Baikov, *Explicit solutions of the multiloop integral recurrence relations and its application*, *Nucl. Instrum. Meth. A* **389** (1997) 347 [[hep-ph/9611449](#)].
- [38] S. Mizera, *Scattering Amplitudes from Intersection Theory*, *Phys. Rev. Lett.* **120** (2018) 141602 [[1711.00469](#)].
- [39] P. Mastrolia and S. Mizera, *Feynman Integrals and Intersection Theory*, *JHEP* **02** (2019) 139 [[1810.03818](#)].
- [40] H. Frellesvig, F. Gasparotto, S. Laporta, M.K. Mandal, P. Mastrolia, L. Mattiazzi et al., *Decomposition of Feynman Integrals on the Maximal Cut by Intersection Numbers*, *JHEP* **05** (2019) 153 [[1901.11510](#)].
- [41] H. Frellesvig, F. Gasparotto, M.K. Mandal, P. Mastrolia, L. Mattiazzi and S. Mizera, *Vector Space of Feynman Integrals and Multivariate Intersection Numbers*, *Phys. Rev. Lett.* **123** (2019) 201602 [[1907.02000](#)].
- [42] S. Mizera and A. Pokraka, *From Infinity to Four Dimensions: Higher Residue Pairings and Feynman Integrals*, *JHEP* **02** (2020) 159 [[1910.11852](#)].
- [43] S. Weinzierl, *On the computation of intersection numbers for twisted cocycles*, [2002.01930](#).
- [44] H. Frellesvig, F. Gasparotto, S. Laporta, M.K. Mandal, P. Mastrolia, L. Mattiazzi et al., *Decomposition of Feynman Integrals by Multivariate Intersection Numbers*, *JHEP* **03** (2021) 027 [[2008.04823](#)].
- [45] A.B. Goncharov, *Multiple polylogarithms, cyclotomy and modular complexes*, *Math. Res. Lett.* **5** (1998) 497 [[1105.2076](#)].
- [46] M. Besier, D. Van Straten and S. Weinzierl, *Rationalizing roots: an algorithmic approach*, *Commun. Num. Theor. Phys.* **13** (2019) 253 [[1809.10983](#)].
- [47] M. Besier, P. Wasser and S. Weinzierl, *RationalizeRoots: Software Package for the Rationalization of Square Roots*, *Comput. Phys. Commun.* **253** (2020) 107197 [[1910.13251](#)].
- [48] C.W. Bauer, A. Frink and R. Kreckel, *Introduction to the GiNaC framework for symbolic computation within the C++ programming language*, *J. Symb. Comput.* **33** (2002) 1 [[cs/0004015](#)].
- [49] J. Vollinga, *GiNaC: Symbolic computation with C++*, *Nucl. Instrum. Meth. A* **559** (2006) 282 [[hep-ph/0510057](#)].
- [50] J. Vollinga and S. Weinzierl, *Numerical evaluation of multiple polylogarithms*, *Comput. Phys. Commun.* **167** (2005) 177 [[hep-ph/0410259](#)].
- [51] L. Naterop, A. Signer and Y. Ulrich, *handyG —Rapid numerical evaluation of generalised polylogarithms in Fortran*, *Comput. Phys. Commun.* **253** (2020) 107165 [[1909.01656](#)].
- [52] S. Borowka, G. Heinrich, S. Jahn, S.P. Jones, M. Kerner, J. Schlenk et al., *pySecDec:*

- a toolbox for the numerical evaluation of multi-scale integrals*, *Comput. Phys. Commun.* **222** (2018) 313 [[1703.09692](#)].
- [53] T. Hahn, *Generating Feynman diagrams and amplitudes with FeynArts 3*, *Comput. Phys. Commun.* **140** (2001) 418 [[hep-ph/0012260](#)].
- [54] A. Djouadi and P. Gambino, *Electroweak gauge bosons selfenergies: Complete QCD corrections*, *Phys. Rev. D* **49** (1994) 3499 [[hep-ph/9309298](#)].
- [55] S. Dittmaier, A. Huss and C. Schwinn, *Dominant mixed QCD-electroweak  $O(\alpha_s\alpha)$  corrections to Drell–Yan processes in the resonance region*, *Nucl. Phys. B* **904** (2016) 216 [[1511.08016](#)].
- [56] PARTICLE DATA GROUP collaboration, *Review of Particle Physics*, *PTEP* **2020** (2020) 083C01.